

# Highly Luminescent Eu<sup>3+</sup> Chelate Nanoparticles Prepared by a Reprecipitation–Encapsulation Method

Hongshang Peng,<sup>†,‡</sup> Changfeng Wu,<sup>‡</sup> Yunfei Jiang,<sup>‡</sup> Shihua Huang,<sup>†</sup> and Jason McNeill<sup>\*,‡</sup>

Key Laboratory of Luminescence and Optical Information, Ministry of Education, Institute of Optoelectronic Technology, Beijing Jiaotong University, Beijing 100044, China, and Department of Chemistry, Center for Optical Materials Science and Engineering Technologies, Clemson University, Clemson, South Carolina 29634

Received October 4, 2006. In Final Form: December 20, 2006

Aqueous suspensions of highly luminescent Eu<sup>3+</sup> chelate nanoparticles are prepared by a novel reprecipitation–encapsulation method. An alkyl alkoxysilane encapsulation agent is included during the nanoparticle formation process, forming a nanoparticle encapsulation layer that inhibits aggregation as evidenced by UV–vis spectroscopy and atomic force microscopy. In addition, the encapsulated nanoparticles exhibit a small size (10 nm), intense luminescence, and excellent photostability. We estimate that the molar extinction coefficients of the ~10 nm particles are approximately  $5.0 \times 10^7 \text{ M}^{-1} \text{ cm}^{-1}$  with a luminescence quantum yield of 6%, indicating a luminescence brightness many times larger than that of conventional fluorescent dyes and comparable to that of colloidal semiconductor quantum dots. The small size, high brightness, highly red-shifted luminescence, and long luminescence lifetimes of the nanoparticles are of interest for luminescence labeling and sensing applications.

## Introduction

Trivalent lanthanide (Ln<sup>3+</sup>) chelates have a number of useful spectroscopic characteristics such as near-UV excitation, sharp emission peaks, highly red-shifted luminescence, and long luminescence lifetimes.<sup>1–3</sup> These characteristics can provide very low detection limits and enhanced sensitivity in luminescence-based detection schemes. For biological applications such as in vivo sensing and imaging, the Ln<sup>3+</sup> chelates must be soluble, stable, free of nonspecific interactions, and sufficiently bright in aqueous solution. However, the luminescence quantum yield of Ln<sup>3+</sup> chelates is usually reduced substantially as a result of quenching by water molecules.<sup>4,5</sup> In certain cases, they also suffer from nonspecific interactions with various cations (such as Ca<sup>2+</sup> and Zn<sup>2+</sup>) and anions (hydroxide and phosphate).<sup>6,7</sup> Therefore, much effort has been devoted to developing luminescent Ln<sup>3+</sup> chelates with improved stability and quantum yield.<sup>8–12</sup> As an alternative, silica or polystyrene nanoparticles containing Ln<sup>3+</sup> chelates have been prepared for biological assays.<sup>13–15</sup> In

comparison with free Ln<sup>3+</sup> chelate molecules, the luminescence brightness of chelate nanoparticles is greatly enhanced because there are many chelate molecules per particle. Furthermore, the Ln<sup>3+</sup> chelates are stabilized by the nanoparticle matrix. However, a shortcoming of these nanoparticles is their large size (>40 nm), which limits their potential applications, particularly for FRET-based detection schemes such as molecular beacons. Inorganic nanoparticles containing Ln<sup>3+</sup> ions have also been developed as potential bioprobes,<sup>16–18</sup> though the small absorption cross section of Ln<sup>3+</sup> ions, large particle size, and broad size range limit their utility for many applications.

Various organic nanoparticles based on fluorescent dyes<sup>19,20</sup> and conjugated polymers<sup>21–23</sup> have been prepared by reprecipitation methods. Recently, Mirkin et al. demonstrated the preparation of colloidal particles of polymeric transition-metal chelates with particle sizes ranging from submicrometer to micrometer.<sup>24</sup> In this letter, smaller Eu<sup>3+</sup> chelate nanoparticles are prepared by a reprecipitation–encapsulation method. In the absence of an encapsulation agent, Eu<sup>3+</sup> chelate particles prepared by reprecipitation are observed to aggregate over the period of a few hours and also exhibit a notable reduction in luminescence. We demonstrate that the addition of an encapsulating agent (octyltrimethoxysilane; OTS) results in stable nanoparticle dispersions that exhibit strong luminescence with a quantum yield even higher than that of the Eu<sup>3+</sup> chelate dissolved in an organic solvent. The resulting nanoparticles have an average

\* Corresponding author. E-mail: mcneill@clemson.edu.

<sup>†</sup> Beijing Jiaotong University.

<sup>‡</sup> Clemson University.

(1) Saha, A. K.; Kross, K.; Kloszewski, E. D.; Upson, D. A.; Toner, J. L.; Snow, R. A.; Black, C. D. V.; Desai, V. C. *J. Am. Chem. Soc.* **1993**, *115*, 11032–11033.

(2) Seveus, L.; Vaisala, M.; Hemmila, I.; Kojola, H.; Roomans, G. M.; Soini, E. *Microsc. Res. Tech.* **1994**, *28*, 149–154.

(3) Xiao, M.; Selvin, P. R. *J. Am. Chem. Soc.* **2001**, *123*, 7067–7073.

(4) Sammes, P. G.; Yahiroglu, G. *Nat. Prod. Rep.* **1996**, *13*, 1–28.

(5) Beeby, A.; Clarkson, I. M.; Dickins, R. S.; Faulkner, S.; Parker, D.; Royle, L.; de Sousa, A. S.; Williams, J. A. G.; Woods, M. *J. Chem. Soc., Perkin Trans. 2* **1999**, 493–503.

(6) Sarka, L.; Burai, L.; Brucher, E. *Chem.—Eur. J.* **2000**, *6*, 719–724.

(7) Liu, S.; Edwards, D. S. *Bioconjugate Chem.* **2001**, *12*, 7–34.

(8) Petoud, S.; Cohen, S. M.; Bunzli, J. C. G.; Raymond, K. N. *J. Am. Chem. Soc.* **2003**, *125*, 13324–13325.

(9) Yang, C.; Fu, L. M.; Wang, Y.; Zhang, J. P.; Wong, W. T.; Ai, X. C.; Qiao, Y. F.; Zou, B. S.; Gui, L. L. *Angew. Chem., Int. Ed.* **2004**, *43*, 5010–5013.

(10) Quici, S.; Cavazzini, M.; Marzanni, G.; Accorsi, G.; Armaroli, N.; Ventura, B.; Barigelletti, F. *Inorg. Chem.* **2005**, *44*, 529–537.

(11) Quici, S.; Marzanni, G.; Cavazzini, M.; Anelli, P. L.; Botta, M.; Gianolio, E.; Accorsi, G.; Armaroli, N.; Barigelletti, F. *Inorg. Chem.* **2002**, *41*, 2777–2784.

(12) Huhtinen, P.; Kivela, M.; Kuronen, O.; Hagren, V.; Takalo, H.; Tenhu, H.; Lovgren, T.; Harna, H. *Anal. Chem.* **2005**, *77*, 2643–2648.

(13) Hemmila, I.; Laitala, V. *J. Fluoresc.* **2005**, *15*, 529–542.

(14) Soukka, T.; Harna, H.; Paukkunen, J.; Lovgren, T. *Anal. Chem.* **2001**, *73*, 2254–2260.

(15) Ye, Z. Q.; Tan, M. Q.; Wang, G. L.; Yuan, J. L. *Anal. Chem.* **2004**, *76*, 513–518.

(16) Boyer, J. C.; Vetrone, F.; Cuccia, L. A.; Capobianco, J. A. *J. Am. Chem. Soc.* **2006**, *128*, 7444–7445.

(17) Diamante, P.; Veggel, F. v. J. *Fluoresc.* **2005**, *15*, 543–551.

(18) Wang, L. Y.; Yan, R. X.; Hao, Z. Y.; Wang, L.; Zeng, J. H.; Bao, H.; Wang, X.; Peng, Q.; Li, Y. D. *Angew. Chem., Int. Ed.* **2005**, *44*, 6054–6057.

(19) Xiao, D. B.; Lu, X.; Yang, W. S.; Fu, H. B.; Shuai, Z. G.; Fang, Y.; Yao, J. N. *J. Am. Chem. Soc.* **2003**, *125*, 6740–6745.

(20) Peng, A. D.; Xiao, D. B.; Ma, Y.; Yang, W. S.; Yao, J. N. *Adv. Mater.* **2005**, *17*, 2070–2073.

(21) Szymanski, C.; Wu, C. F.; Hooper, J.; Salazar, M. A.; Perdomo, A.; Dukes, A.; McNeill, J. *J. Phys. Chem. B* **2005**, *109*, 8543–8546.

(22) Wu, C.; Szymanski, C.; McNeill, J. *Langmuir* **2006**, *22*, 2956–2960.

(23) Wu, C.; Peng, H.; Jiang, Y.; McNeill, J. *J. Phys. Chem. B* **2006**, *110*, 14148–14154.

(24) Oh, M.; Mirkin, C. A. *Nature* **2005**, *438*, 651–654.

size of 10 nm, from which it is estimated that each particle contains  $\sim 1000$   $\text{Eu}^{3+}$  chelate molecules. On the basis of the stability, high luminescence brightness, and small size of these nanoparticles, they are very promising for demanding applications such as luminescent labels or ultrasensitive assays.

### Experimental Section

The  $\text{Eu}^{3+}$  chelate, Eu-tris(dibenzoylmethane)-mono(triphenylphosphineoxide) ( $\text{Eu}(\text{DBM})_3\text{TPPO}$ ) was prepared as described elsewhere.<sup>25</sup> Nanoparticle suspensions of the chelate were prepared by a reprecipitation–encapsulation method that is described as follows: Solid  $\text{Eu}(\text{DBM})_3\text{TPPO}$  was dissolved in tetrahydrofuran (THF, 99.9%, Aldrich) to a concentration of 0.05 wt %. Encapsulating agent octyl trimethoxysilane (OTS) was added to the chelate solution at the OTS to a  $\text{Eu}(\text{DBM})_3\text{TPPO}$  molecular ratio of 1:5. The chelate/OTS solution (200  $\mu\text{L}$ ) was injected quickly into 8 mL of distilled water while the mixture was under sonication. Prior to injection, the pH value of the distilled water was adjusted to  $\sim 9$  by adding ammonium hydroxide (28%, Aldrich). The as-prepared samples were filtered through a 0.2  $\mu\text{m}$  membrane filter (Millipore). The THF was removed by partial vacuum evaporation, followed by another filtration through a 0.2  $\mu\text{m}$  filter. Multiple experiments indicate that the preparation method reproducibly produced nanoparticles, with a typical nanoparticle yield of 80–90%. For comparison, additional samples were prepared without the OTS agent, with different OTS concentrations, and with OTS but without ammonium hydroxide.

The morphology and size distribution of the  $\text{Eu}^{3+}$  chelate nanoparticles were characterized by atomic force microscopy (AFM). One drop of the nanoparticle dispersion was placed on a freshly cleaned oxidized silicon substrate. After the evaporation of water, the surface was scanned with a Digital Instruments multimode AFM in tapping mode. The UV–vis absorption spectra were recorded with a Shimadzu UV-2101PC scanning spectrophotometer using a 1 cm quartz cuvette. Steady-state luminescence spectra were collected from the nanoparticle dispersion in a 1 cm quartz cuvette using a commercial fluorometer (Quantamaster, PTI, Inc.). For luminescence quantum yield measurements, a dilute solution of coumarin 1 in ethanol was used as a standard. Both the nanoparticle dispersion and the coumarin 1/ethanol solution were adjusted to have an absorbance of 0.10. The emission spectra were recorded by using the PTI fluorometer. A corrected luminescence integrated area was used to calculate the quantum yield. The photobleaching experiments were done on the same fluorometer that was set to generate continuous UV light (360 nm) at a power of 1.0 mW. The light was focused into a quartz cell containing a constantly stirred nanoparticle dispersion or  $\text{Eu}^{3+}$  chelate in THF solution with an absorbance of 0.10. The luminescence decrease at 613 nm wavelength was recorded in a time period of 2 h. The luminescence decay lifetime was measured using a home-built photon-counting spectrometer. The sample was excited by pulses from a light-emitting diode (370 nm) driven by a programmable function generator (Seintek G5100). Luminescence emission was collected in perpendicular geometry, separated through a 500 nm long-pass filter, and detected by a single photon-counting module (Perkin-Elmer, SPCM-AQR). A digital counter card (National Instruments model 6602) was configured to record photon arrival events at better than 1  $\mu\text{s}$  resolution.

### Results and Discussion

The luminescence of lanthanide ions arises from parity-forbidden 4f–4f transitions that typically exhibit very low extinction coefficients ( $1\text{--}10\text{ M}^{-1}\text{ cm}^{-1}$ ).<sup>26</sup> The extinction coefficients can be effectively increased by the well-known “antenna effect”, whereby organic chromophores coordinated with lanthanide ions serve as antennas to absorb light and then transfer energy to the metal ions.  $\beta$ -Diketone ligands such as

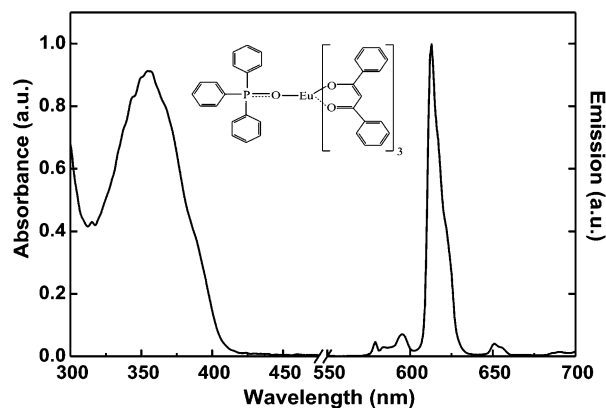


**Figure 1.** UV–vis absorption and emission spectra of  $\text{Eu}(\text{DBM})_3\text{TPPO}$  in THF solution. (Inset) Chemical structure of the  $\text{Eu}(\text{DBM})_3\text{TPPO}$  molecule.

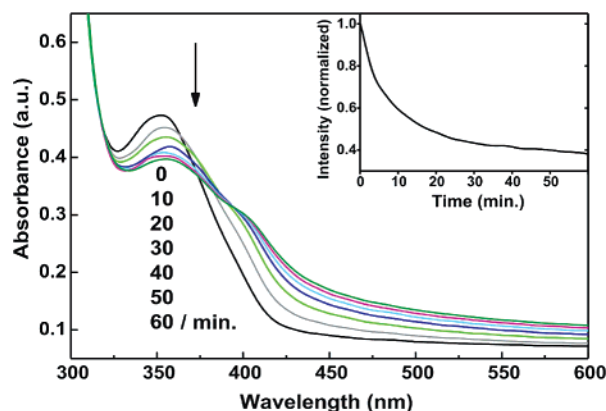


**Figure 2.** Time-dependent UV–vis absorption spectra of a freshly prepared  $\text{Eu}(\text{DBM})_3\text{TPPO}$  pure (without OTS) nanoparticle suspension. The absorption spectra are measured every 10 min, with the sequence indicated by the arrow. (Inset) Time-dependent intensity change of 613 nm emission from the pure  $\text{Eu}(\text{DBM})_3\text{TPPO}$  nanoparticles. Emission intensity is normalized to the initial value.

dibenzoylmethane are often used in lanthanide complexes because of their stable coordination with  $\text{Eu}^{3+}$  ions and strong absorption in the near-UV region.<sup>27,28</sup> Figure 1 presents the chemical structure of  $\text{Eu}(\text{DBM})_3\text{TPPO}$  and the absorption and emission spectra of this chelate in THF solution. The 355 nm absorption band is attributed to the absorption of dibenzoylmethane. The luminescence of the compound is dominated by the forced electric dipole transitions of  $\text{Eu}^{3+}$  ions ( $613\text{ nm}$ ,  $^5\text{D}_0 \rightarrow ^7\text{F}_2$ ), which are sensitive to the ligand field and site symmetry occupied by the  $\text{Eu}^{3+}$  ion.

We have recently demonstrated a facile reprecipitation method for preparing hydrophobic conjugated polymer nanoparticles.<sup>21–23</sup> Here we apply this method to hydrophobic  $\text{Ln}^{3+}$  chelate molecules. After injection of pure  $\text{Eu}(\text{DBM})_3\text{TPPO}/\text{THF}$  solution, the resulting suspension is slightly hazy, exhibiting the characteristic Tyndall effect of colloidal systems. However, it is observed that the suspension slowly becomes faint blue and then white, indicating aggregation to form large particles. To monitor the evolution of the  $\text{Eu}^{3+}$  chelate particle suspension, the evolution of the absorption and luminescence spectra over time was recorded immediately after injection, as shown in Figure 2 and its inset. A bathochromic shift of the 355 nm absorption band is observed as well as the emergence of a lower-energy trailing edge, which is attributable to the presence of aggregates. Figure 2 (inset)

(25) Wang, M.; Jin, L.; Liu, S.; Cai, G.; Huang, J.; Qin, W.; Huang, S. *Sci. China, Ser. B* **1994**, 23, 1028–1034.

(26) Selvin, P. R. *Annu. Rev. Biophys. Biomol. Struct.* **2002**, 31, 275–302.

(27) Zhao, D.; Qin, W. P.; Zhang, J. S.; Wu, C. F.; Qin, G. S.; De, G. J. H.; Zhang, J. S.; Lu, S. Z. *Chem. Phys. Lett.* **2005**, 403, 129–134.

(28) Zhao, D.; Qin, W. P.; Wu, C. F.; Qin, G. S.; Zhang, J. S.; Lu, S. Z. *Chem. Phys. Lett.* **2004**, 388, 400–405.

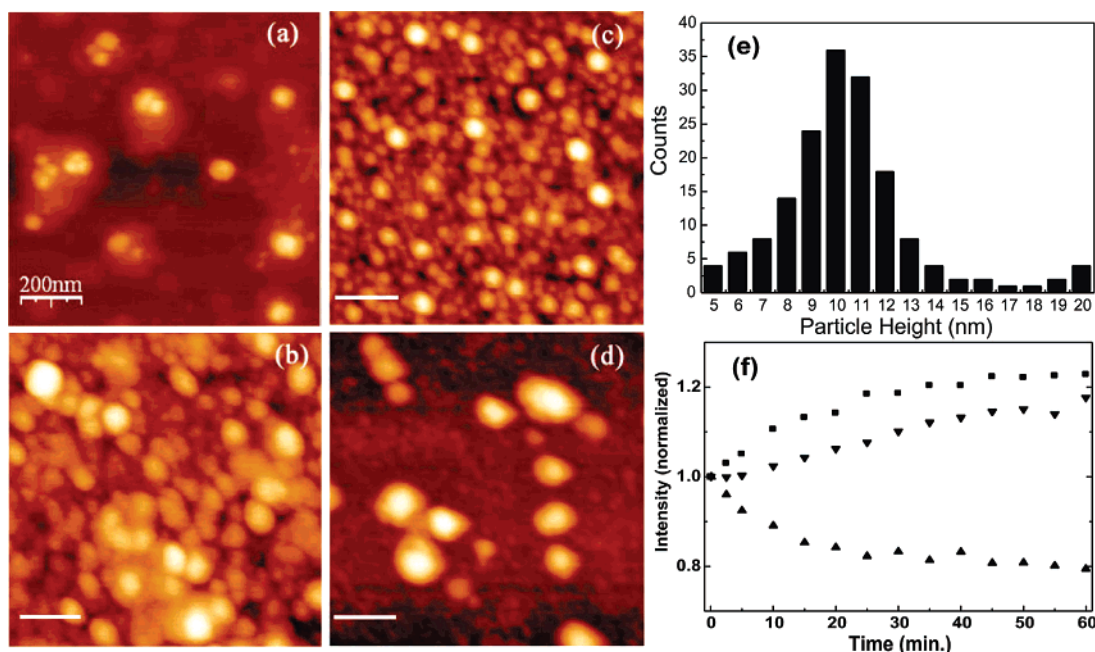


**Figure 3.** AFM images of Eu(DBM)<sub>3</sub>TPPO nanoparticles prepared (a) without OTS and with Eu(DBM)<sub>3</sub>TPPO/OTS nanoparticles with molar ratios of (b) 1:1, (c) 1:5, and (d) 1:10. The scale bar is 200 nm. (e) Histogram of particle height taken on an AFM image with sparsely dispersed nanoparticles (with a 1:5 Eu(DBM)<sub>3</sub>TPPO/OTS ratio). (f) Time dependence of the 613 nm emission intensity of freshly prepared Eu(DBM)<sub>3</sub>TPPO/OTS nanoparticles with varying molar ratios of OTS. Molar ratios of 1:1, 5:1, and 10:1 are respectively labeled as ▲, ▼, and ■. The emission intensity is normalized to the initial value.

indicates the intensity change of 613 nm emission from the freshly prepared bare nanoparticles under continuous UV excitation over the course of 1 h. The luminescence of these bare particles decreases very quickly. The rapid decrease is likely due to one or more of the following mechanisms: dissociation of the Eu<sup>3+</sup> chelate molecules on the exposed cluster surfaces, efficient nonradiative relaxation via coupling to O–H vibrations of water,<sup>4</sup> and rapid photodestruction.

Encapsulated Eu(DBM)<sub>3</sub>TPPO nanoparticles prepared in the presence of OTS exhibit markedly different behavior. The nanoparticle suspensions exhibit stable luminescence and remain transparent for weeks with no apparent aggregation. Tapping mode AFM was used to determine the dependence of nanoparticle morphology on the molar ratio of OTS to Eu(DBM)<sub>3</sub>TPPO (Figure 3). For suspensions prepared without the OTS, the presence of very small particles (likely containing a few molecules) as well as larger aggregates can both be seen in the AFM image (Figure 3a). With the addition of a small amount of OTS (1:1 OTS/Eu(DBM)<sub>3</sub>TPPO molar ratio), the AFM image indicates a somewhat narrower range of particle sizes (Figure 3b). With an increase in the OTS/Eu(DBM)<sub>3</sub>TPPO molar ratio to 5:1, the resulting nanoparticles exhibit a narrower size distribution, with few aggregates visible in the image (Figure 3c). A further increase in the molar ratio to 10:1 leads to larger particles and a large size distribution (Figure 3d). In the current study, it appears that 5:1 is the optimal ratio for the formation of a stable, relatively monodisperse nanoparticle suspension. Height analysis (Figure 3e) performed on an AFM image with sparse particle coverage indicates that the majority of these nanoparticles have a diameter in the range of 5–15 nm. The larger lateral particle size in Figure 3c relative to the particle height is attributed to the tip convolution effect.<sup>29</sup> Evidence of nanoparticle nucleation and growth and the formation of the encapsulating alkoxy silane shell can be observed in the time evolution of the absorption and luminescence spectra

of the freshly prepared Eu(DBM)<sub>3</sub>TPPO suspensions. The absorption spectra of the encapsulated nanoparticles remain unchanged for weeks, consistent with the relatively low occurrence of aggregates observed in the AFM results. However, there are remarkable differences in the luminescence intensity that depend on the OTS/chelate ratio, as shown in Figure 3f. The luminescence intensity of the sample prepared with a 1:1 OTS/chelate ratio is observed to decrease gradually with time. However, for the nanoparticles prepared with higher ratios of OTS (5:1 and 10:1), the luminescence (at 613 nm) is observed to increase over time. These results are consistent with improved isolation of the Eu<sup>3+</sup> ions from water with higher ratios of OTS to chelate. A likely explanation for the gradual increase in intensity is that the adsorption and hydrolysis of the alkoxy silane molecules on the surface of the hydrophobic chelate particles result in the formation of a protecting layer, effectively isolating the Eu<sup>3+</sup> ions from water and thus reducing the deleterious effects of water on the luminescence yield. There may also be some water initially trapped in the nanoparticles upon formation that slowly exits the interior of the nanoparticles by diffusion, possibly accompanied by reorganization and densification of the particles. To test the importance of base-catalyzed hydrolysis of the OTS on nanoparticle stability, we also measured the time evolution of spectra from Eu<sup>3+</sup> chelate/OTS nanoparticles prepared without ammonia. The temporal evolution of both the absorption spectra and the 613 nm emission of the resulting suspension is similar to that of suspensions formed without OTS. This indicates that the rapid hydrolysis of the OTS in a basic environment plays a key role in inhibiting aggregation, perhaps as a result of interparticle electrostatic repulsion due to the negatively charged silica layer. It should also be mentioned that sonication during the mixing step is required for the formation of the nanoparticle suspension. This suggests that rapid mixing due to the formation of microjets in the mixture under sonication is essential for ensuring uniform nucleation and growth of the chelate nanoparticles. Further studies are required to determine how particle size, size range, and stability

(29) Morris, V. J.; Kirby, A. R.; Gunning, A. P. *Atomic Force Microscopy for Biologists*; Imperial College Press: London, 1999.



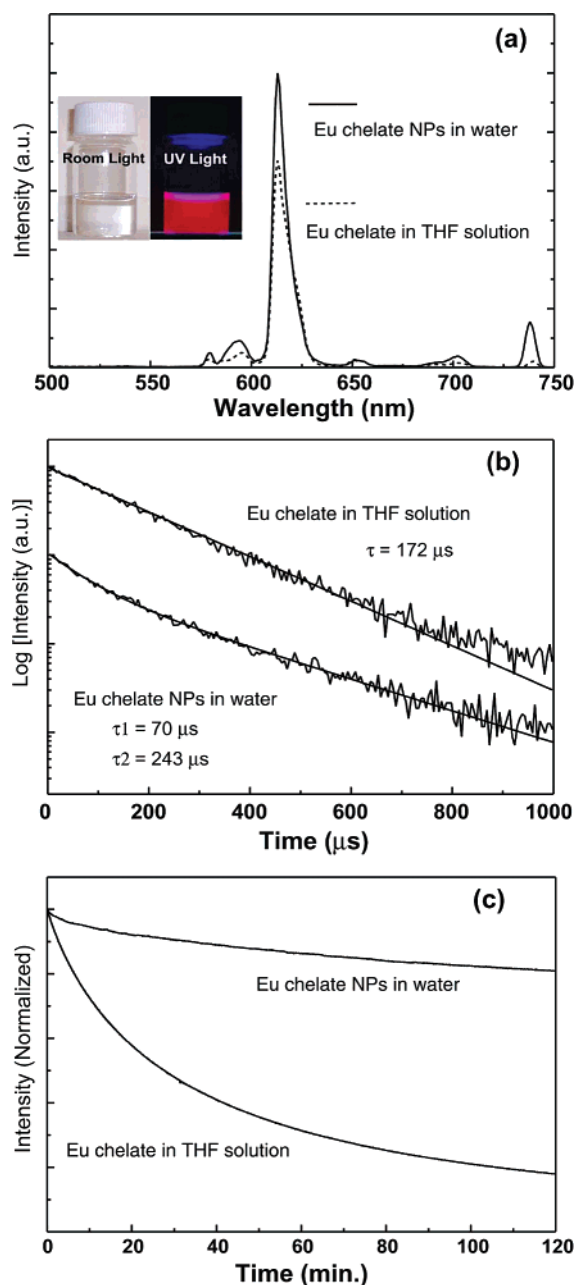


**Figure 4.** (a) Emission spectra, (b) luminescence decay, and (c) photobleaching curves of Eu(DBM)<sub>3</sub>TPPO in THF solution and 5:1 Eu(DBM)<sub>3</sub>TPPO/OTS nanoparticle dispersions. In all cases, the absorbance is adjusted to 0.1. Emission spectra and photobleaching curves were recorded under continuous illumination of 360 nm UV light.

depend on factors such as the kinetics of hydrolysis of OTS, the kinetics of chelate aggregation, the kinetics of adsorption of OTS onto the surface of the particles, interparticle Coulomb forces, and the surface free energy of the particles.

Whereas some batch-to-batch variability in optical properties and particle diameters was observed, we conclude that a stable, relatively monodisperse Eu(DBM)<sub>3</sub>TPPO nanoparticle suspension is obtained in the presence of OTS (with an OTS/Eu(DBM)<sub>3</sub>TPPO molar ratio of 5:1 or weight ratio of 1:1). The remainder of our discussion is focused on the luminescence properties of the particles prepared with a 5:1 OTS/Eu(DBM)<sub>3</sub>TPPO molar ratio and, in particular, their figures of merit for labeling applications. As shown in the inset of Figure 4a, the nanoparticle dispersions are clear and colorless but exhibit strong red luminescence for weeks. To test the long-term stability of the Eu<sup>3+</sup> chelate/OTS

nanoparticles toward aggregation, samples filtered through a 0.2 μm filter after aging for 4 weeks indicated no loss of material, as determined by UV-vis absorption spectroscopy. The molar extinction coefficient of the Eu(DBM)<sub>3</sub>TPPO molecules in THF solution was determined to be  $5.0 \times 10^4 \text{ M}^{-1} \text{ cm}^{-1}$  at 350 nm. Assuming the nanoparticles to have an average size of 10 nm, it is estimated that each particle contains  $\sim 1000 \text{ Eu}^{3+}$  chelate molecules, yielding a nanoparticle molar extinction coefficient of  $\sim 5 \times 10^7 \text{ M}^{-1} \text{ cm}^{-1}$  at 350 nm, which is much higher than that of conventional fluorescent dyes and semiconducting quantum dots.<sup>30</sup> It should be noted that a unique feature of the nanoparticles is that such a large number of Ln<sup>3+</sup> chelate molecules are contained in such a small particle. The photoluminescence quantum yield of the Ln<sup>3+</sup> chelate molecules is not observed to decrease in the nanoparticles relative to dilute solution, despite the high concentration of Ln<sup>3+</sup> chelate molecules within the particles, in contrast to many conventional organic fluorescent dyes that exhibit self-quenching at high concentrations. This is due to the nature of the Ln<sup>3+</sup> excited state, which is largely isolated from the influence of nearby atoms, and the presence of the ligands, which effectively separate the Ln<sup>3+</sup> ions.<sup>8–13</sup> A luminescence quantum yield of 6% was measured for the Eu(DBM)<sub>3</sub>TPPO/OTS nanoparticles using a dilute solution of Coumarin 1 in ethanol as a standard. The quantum yield of the encapsulated Eu(DBM)<sub>3</sub>TPPO nanoparticles is approximately 30% higher than that of the chelate in THF solution. A similar increase in luminescence yield for silica host doped with Eu<sup>3+</sup> chelates as compared to pure chelate has been reported previously<sup>28,31</sup> and is attributable to a reduction in the number of vibrational modes that couple to nonradiative transitions. The luminescence brightness is defined as the product of the molar absorption coefficient and the quantum yield. On the basis of the large absorptivity and quantum yield of these nanoparticles, the calculated luminescence brightness is many times larger than that of conventional fluorescent dyes and comparable to that of colloidal semiconductor quantum dots.<sup>32</sup>

The luminescence decay curves of the Eu<sup>3+</sup> chelate in THF solution and encapsulated nanoparticles are presented in Figure 4b. The luminescence decay of the chelate in THF solution corresponds to a single-exponential function with a time constant of 172 μs. The luminescence decay of the nanoparticles does not fit to a single-exponential function, whereas a biexponential function yields a good fit with time constants of 70 μs (60% amplitude) and 243 μs (40% amplitude). A similar biexponential decay was observed in silica spheres containing a similar Eu<sup>3+</sup> chelate and is attributable to site-to-site heterogeneity in the solid state.<sup>27,28</sup> The decreased lifetime and increased quantum yield were also observed in Eu<sup>3+</sup> chelate-loaded silica spheres as compared to pure chelate and were attributed to an increase in the radiative rate.<sup>27,28</sup> Photostability is another key figure of merit for luminescent probes. The decay of the luminescence of both the Eu<sup>3+</sup> chelate in THF solution and the encapsulated nanoparticles under continuous UV light illumination was determined (Figure 4c). It was observed that the emission intensity of the Eu<sup>3+</sup> chelate in THF solution decreased by approximately 80% over the course of 2 h whereas the emission intensity of the Eu<sup>3+</sup> chelate/OTS nanoparticles showed only a slight decrease ( $\sim 10\%$ ) over the same period, corresponding to a decrease in the photobleaching rate by a factor of 20. The high photostability of the encapsulated nanoparticles may be due to the isolation of

(30) Leatherdale, C. A.; Woo, W. K.; Mikulec, F. V.; Bawendi, M. G. *J. Phys. Chem. B* **2002**, *106*, 7619–7622.

(31) Ji, X. L.; Li, B.; Jiang, S. C.; Dong, D. W.; Zhang, H. J.; Jing, X. B.; Jiang, B. Z. *J. Non-Cryst. Solids* **2000**, *275*, 52–58.

(32) Hohng, S.; Ha, T. *ChemPhysChem* **2005**, *6*, 956–960.

the  $\text{Eu}^{3+}$  chelate from the outside environment by a layer of hydrolyzed OTS, which would shield the chelate from solvent molecules and free radicals caused by light exposure and effectively protecting the molecules from photodecomposition.

### Conclusions

In summary, encapsulated nanoparticles of a rare earth chelate were prepared by a reprecipitation–encapsulation method. The presence of an encapsulation agent in the preparation mixture results in aqueous nanoparticle suspensions that are stable, with a small particle size ( $\sim 10$  nm), and little evidence of precipitation or the formation of large aggregates. Encapsulation by base-catalyzed hydrolysis of OTS and subsequent formation of a protecting layer on the nanoparticle surface are shown to stabilize the suspension against particle aggregation and protect the  $\text{Eu}^{3+}$  chelate from photodestruction and luminescence quenching by water. The high nanoparticle molar extinction coefficient, estimated to be  $\sim 5 \times 10^7 \text{ M}^{-1}\text{cm}^{-1}$ , and the luminescence

quantum yield of 6% indicate per particle luminescence brightness figures rivaling those of quantum dots and organic dye-loaded spheres of similar dimensions. The brightness, photostability, and long luminescence lifetime of these nanoparticles are promising for demanding applications such as luminescent labels and ultrasensitive assays. In addition, the reprecipitation–encapsulation method that we have demonstrated may also be applied for the preparation and encapsulation of other hydrophobic metal complex nanoparticles.

**Acknowledgment.** We are grateful to Professor Linpei Jin for providing the solid  $\text{Eu}(\text{DBM})_3\text{TPPO}$  and Dr. Dvora Perahia for her assistance with AFM measurements. This work was supported by NSF-EPSCoR, an NSF Career Award (0547846), the EDSTIF of Beijing Jiaotong University (48001), and the National Natural Science Foundation of China (10374002).

LA062915I